ISSN (Print) 1226-1750
ISSN (Online) 2233-6656
Journal of Magnetics 18(4), 466-472 (2013) http://dx.doi.org/10.4283/JMAG.2013.18.4.466

Shorted Turn in the Hybrid Magnet Engine Valve Actuator for Enhanced Dynamic Performance

Hwa Cho Yi[1], Ki Il Hwang[2], Jihun Kim[3], and Jin Ho Kim[1]*

[1]*Shool of Mechanical Engineering, Yeungnam University, Gyengbuk, Korea*
[2]*LG Electronics, Changwon, Gyengnam, Korea*
[3]*Korea Aerospace Research Institute, Daejeon, Korea*

(Received 5 September 2013, Received in final form 9 November 2013, Accepted 23 November 2013)

This paper presents a new design of the hybrid magnet engine valve actuator using the shorted turn for enhanced dynamic performance. The quick response of coil electric current is the most important factor that determines the opening and closing performance of the hybrid magnet engine valve. The conventional hybrid magnet engine valve actuator, however, has a delayed initial electric current rising when it is driven by voltage control because of the coil inductance which is a typical characteristic of an electromagnetic coil. A shorted turn is newly placed into the upper yoke of the hybrid magnet engine valve actuator to reduce coil inductance and thus, to hasten the initial electric current rising. We performed a dynamic finite element analysis to demonstrate the improvement of the dynamic characteristics of the hybrid magnet engine valve actuator due to the shorted turn.

Keywords : flat coil actuator, shorted turn, center pole, inductance, lumped parameter analysis, experiment

1. Introduction

Variable valve timing (VVT) is the key technology to enhance the performance of internal combustion engine by allowing the valve events to be independent of camshaft rotation. As a result, fuel consumption may be reduced up to 15%, torque output enhanced for wide range of engine speeds, and CO_2 emission decreased up to 15% [1, 2].

In the past years, the mechanical and hydraulic actuators had been used for VVT. The simplest VVT systems advance or retard the timing of the intake or exhaust valves, like Mazda's S-VT. On the other hand, Honda's VTEC switches between two sets of cams at a certain engine revolution per minute (RPM) [3, 4]. These systems, however, have inherent drawbacks such as the limited flexibility of valve timing and heavy weight.

The hybrid magnet engine valve actuator using a permanent magnet and an electromagnet (PM/EM) is one of the most advanced VVT systems. Fig. 1 shows the schematic diagram of the hybrid magnet engine valve actuator. It consisted of two permanent magnets, an electromagnetic coil, a laminated steel core with an armature, two springs and a valve body. The main operation principle is based on mass-spring oscillation, and the VVT is achieved by controlling the voltage applied to the coils [5]. This actuator

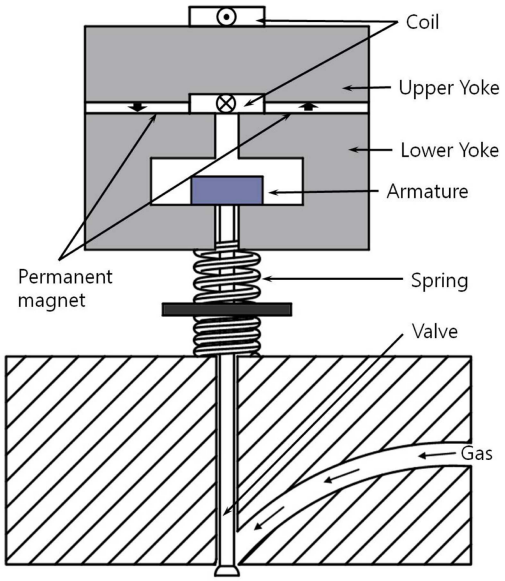

Fig. 1. (Color online) Schematic diagram of the conventional hybrid magnet engine valve.

*Corresponding author: Tel: +82-53-810-2441
Fax: +82-53-810-4627, e-mail: jinho@ynu.ac.kr

driven by voltage control, however, has high electromagnetic coil inductance, which retards the valve release and lengthens the valve transition time, negatively affecting the dynamic performance of the actuator.

One of the ways to reduce the high inductance of the electromagnetic coil is a shorted turn. In the early 1980s, the dynamic performance of the dual path voice coil motor was improved by wrapping its yoke with a thin copper plate, called "Shorted Turn", which induces the rapid increase of the coil electric current [6-8].

In this paper, the new design of the hybrid magnet engine valve actuator uses the shorted turn to generate a fast electric current rising. To analyze the proposed design mathematically, we performed a lumped parameter analysis and dynamic finite element analysis to demonstrate the improvement of the dynamic characteristics of the hybrid actuator, especially the fast electric current rising characteristic.

2. Structure and Operating Principle

2.1. Structure of the proposed actuator

In order to reduce the inductance of the electromagnetic coil, the upper yoke of the actuator is wrapped by a thin copper plate, as shown in Fig. 2. The thin copper plate is known as "shorted turn," which helps the electric current of the coil to rise quickly. When voltage is applied to the coil, the flux in the magnetic circuit induces a high electric current in the copper sleeve that retards the increase of the magnetic flux. As a result, the inductance of the coil is reduced and the electric current rises quickly [9].

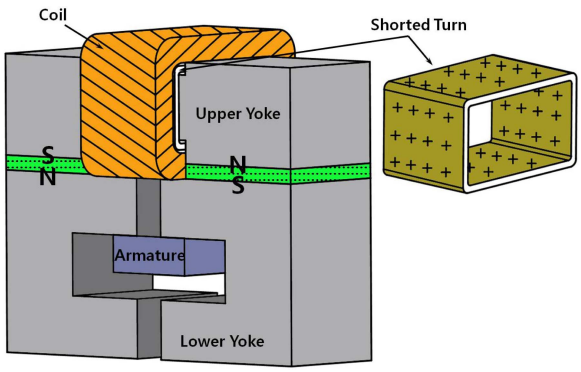

Fig. 2. (Color online) Schematic diagram of proposed hybrid magnet engine valve actuator.

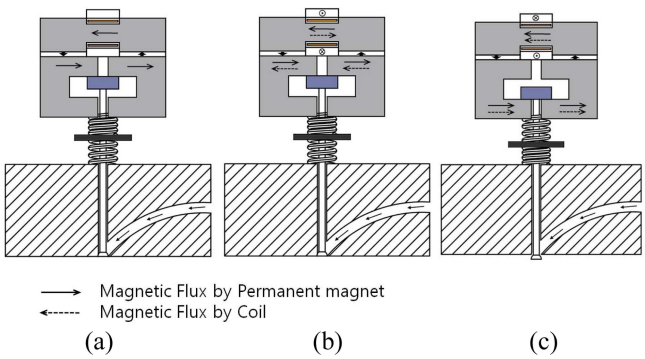

Fig. 3. (Color online) Principle of operation with the armature at the (a) upper end, (b) initial position and (c) at lower end.

2.2. The operating principle

Fig. 3 shows the operating principle of the actuator. Initially, the armature is held at the upper end since the magnetic force is greater than the spring force (Fig. 2a). The armature is released when the coil is energized by applied voltage and cancels the flux from the permanent magnet. The shorted turn helps the coil electric current to rise quickly, resulting in faster decrease of the magnetic latching force. The spring force then becomes greater than the magnetic force and the springs accelerate the armature downward using the stored potential energy (Fig. 2b). In short, the shorted turn induces a faster release of the armature from the upper end. In the neutral position, the coil is energized by the applied voltage to have the same flux flow as the permanent magnet. The magnetic force from both the coil and the permanent magnet overcomes the spring force, and the armature is held at the lower end, so the valve is fully opened (Fig. 2c). These events occur successively. The total traveling distance of the armature is 7.8 mm. Transition time is defined as the duration in which the valve moves from the closed position to the open position or from the open position to the closed position. As the transition time becomes smaller, higher flexible valve timing is achieved. By controlling the voltage of the electromagnetic coil, we can control the holding time of the armature and, as a result, realize VVT [10].

3. Lumped Parameter Analysis

Lumped parameter analysis, an alternative to finite element analysis, is popular for its accuracy and quick computational iterations [11]. To verify the faster rise of the electric current in coil due to the shorted turn, lumped parameter models of the conventional actuator and the proposed actuator with shorted turn were created.

3.1. Conventional actuator

The coil magnetic flux pattern in the conventional hybrid magnet engine valve actuator is shown in Fig. 4. The induced Faraday voltage in the coil is presented by Eq. (1) as follows.

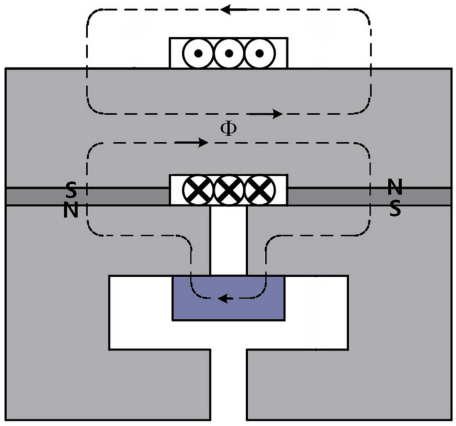

Fig. 4. (Color online) Lumped parameter model of the conventional actuator.

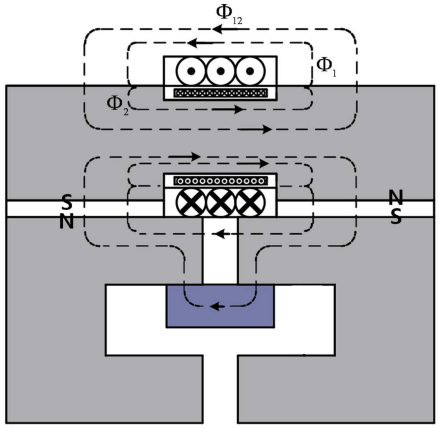

Fig. 5. (Color online) Lumped model of the proposed hybrid magnet engine valve actuator with shorted turn.

$$e = N\frac{d\Phi}{dt} \tag{1}$$

Where:

e is the induced voltage in coil.
N is the number of turns in the coil.
Φ is the mutual flux.

The applied voltage source and the magneto motive force can be expressed by Eqs. (2) and (3) by Kirchhoff's law and magnetic Ampere's law.

$$V = Ri + e \tag{2}$$

$$Ni = \frac{\Phi}{P} \tag{3}$$

Where:

V is the applied voltage source.
R is the coil resistance.
i is the electric current in coil.
P is the leakage permeance of the Φ loop.

Combining Eq. (3) with Eq. (1) gives Eq. (4), and then Eq. (4) is combined with Eq. (2) to give Eq. (5). Permeance of the magnetic flux can be expressed by Eq. (7).

$$e = N\frac{d[PNi]}{dt} \tag{4}$$

$$V = Ri + N\frac{d[PNi]}{dt} \tag{5-a}$$

$$V = Ri + L\frac{di}{dt} \tag{5-b}$$

$$L = N^2P \tag{6}$$

$$P = P_{yoke\_without} + P_{PM} + P_{armature} \tag{7}$$

Where:

$P_{yoke\_without}$ is the permeance of the yoke of the conventional actuator (Wb/AT)
P_{PM} is the permeance of the permanent magnet (Wb/AT)
$P_{armature}$ is the permeance of the armature (Wb/AT)

From the Eq. (5-b), the asymptotic final electric current value of the conventional actuator can be expressed by Eq. (8).

$$i_{conventional} = \frac{V}{R} \tag{8}$$

3.2. Proposed actuator

Fig. 5 shows the lumped parameter models of the new hybrid magnet engine valve actuator with the shorted turn. The magnetic fluxes are generated by the coil and the shorted turn. When voltage is applied to the coil, the transient electric current i_1 flows in the coil and induces a transient electric current flow i_2 in shorted turn in the opposite direction. In following Faraday's law, the induced voltages in the coil and shorted turn are expressed by Eqs. (9) and (10), respectively.

$$e_1 = N_1\frac{d(\Phi_{12} + \Phi_1)}{dt} \tag{9}$$

$$e_2 = N_2\frac{d(\Phi_{12} + \Phi_2)}{dt} \tag{10}$$

Where:

e_1 is the induced voltage in coil (V)
e_2 is the induced voltage in the shorted turn (V)
N_1 is the number of turn in the coil (turns)
N_2 is the number of turn in the shorted turn (turns)
Φ_1 is the leakage flux unique to coil only (Wb)

Φ_2 is the leakage flux unique to shorted turn only (Wb)
Φ_{12} is the mutual flux, linking both coil and shorted turn (Wb)

The applied voltage to the coil and the shorted turn can be expressed by Eqs. (11) and (12) following Kirchoff's law and Ohm's law, respectively.

$$V_1 = R_1 i_1 + e_1 \tag{11}$$

$$0 = R_2 i_2 + e_2 \tag{12}$$

Where:

V_1 is the applied voltage (V)
R_1 is the coil resistance (Ω)
R_2 is the shorted turn resistance (Ω)
i_1 is the electric current in coil (A)
i_2 is the electric current in shorted turn (A)

Also, the magnetic force is expressed by Ampere's law as in the following Eqs. (13), (14) and (15).

$$N_1 i_1 + N_2 i_2 = \frac{\phi_{12}}{P_{12}} \tag{13}$$

$$N_1 i_1 = \frac{\phi_1}{P_1} \tag{14}$$

$$N_2 i_2 = \frac{\phi_2}{P_2} \tag{15}$$

Where:

P_1 is the leakage permeance of the Φ_1 loop (Wb/AT)
P_2 is the leakage permeance of the Φ_2 loop (Wb/AT)
P_{12} is the leakage permeance of the Φ_{12} loop (Wb/AT)

Combining theses equations from Eq. (9) to Eq. (15) results in Eqs. (16) and (17).

$$V_1 = R_1 i_i + (L_{12} + L_1)\frac{di_1}{dt} + L_{12}\frac{di_2^*}{dt} \tag{16}$$

$$0 = R_2^* i_2^* + L_{12}\frac{di_1}{dt} + (L_{12} + L_2)\frac{di_2^*}{dt} \tag{17}$$

Where, $i_2^* = \frac{N_2}{N_1} i_2$ and $R_2^* = \left(\frac{N_1}{N_2}\right)^2 R_2$

$$L_1 = N_1^2 P_1 \text{ with } P_1 = \frac{\mu_0 \cdot A_{coil}}{l_{coil}} \tag{18}$$

$$L_2 = N_1^2 P_2 \text{ with } P_2 = \frac{\mu_0 \cdot A_{shorted}}{l_{shorted}} \tag{19}$$

$$\text{with } P_{12} = P_{yoke\_with} + P_{PM} + P_{armature} \tag{20}$$

Where:

P_{yoke_with} is the permeance of the yoke of the proposed actuator (Wb/AT)
L_1 is the leakage inductance as seen by P_1 (H)
L_2 is the leakage inductance as seen by P_2 (H)
L_{12} is the mutual inductance as seen by P_{12} (H)
l_{coil} is the effective length of the coil (mm)
$l_{shorted}$ is the effective length of the shorted turn (mm)
A_{coil} is the cross-section area of Φ_1 path (mm)
$A_{shorted}$ is the cross-section area of Φ_2 path (mm)

Table 1. Lumped model parameters.

N	250 (turns)	N_1	250 (turns)
N_2	1 (turn)	R	0.8886(Ω)
R_1	0.8886 (Ω)	R_2	0.73731×10^{-6}(Ω)
V	30 (V)	V_1	30 (V)
L	8.5(mH)	L_1	1.187(mH)
L_2	1.046(mH)	L_{12}	8.24(mH)

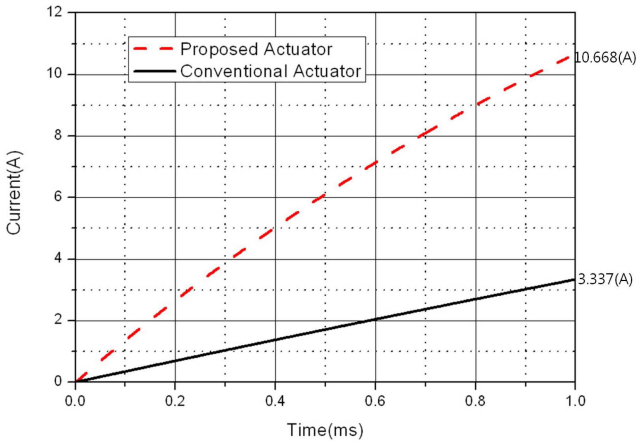

Fig. 6. (Color online) Comparison of coil electric current versus time between the models of the conventional actuator and the proposed actuator with shorted turn, respectively. by lumped parameter analysis.

Equation (7) and the coupled Eqs. (16) and (17) were solved to obtain the electric current responses of the conventional actuator and the proposed actuator with the shorted turn, as shown in Fig. 6. The rate of electric current increase of the proposed flat coil actuator is about three times higher than that of the conventional flat coil actuator at 1 ms. This simulation is performed assuming that that the armature is stationary and so, the speedance is neglected.

4. Dynamic Finite Element Analysis

Finite-element models (FEM) were created and dynamic finite-element analysis was performed using the nonlinear FEM solver Maxwell. The newly proposed actuator was composed of three subsystems: a mechanical system, an

Table 2. The magnetic properties of NdFE35 permanent magnet.

Symbol	Magnetitude
B_r (T)	1.10
Hc (A/m)	-8.38×10^5
μ	1.044573

electrical system, and a magnetic system, which are all coupled.

The magnetic subsystem is governed by Eq. (21). The nonlinear magnetic B-H properties of steel1010 were assigned to the yokes and the armature, and the magnetic properties of NdFe35 were assigned to the permanent magnet. Table 2 shows the specifications of the NdFe35 permanent magnet.

$$\nabla \times \left(\frac{1}{\mu} \nabla \times \vec{A}_z \right) = \vec{J}_{ext} + \frac{1}{\mu} \nabla \times \vec{M} \tag{21}$$

Boundary condition $\vec{A}_z = 0$
$\vec{A}_z$ is the magnetic vector potential
$\vec{J}_{ext}$ is the external electric current density
μ is the permeability of the material
$\vec{M}$ is the magnetization of the permanent magnet

The mechanical system is governed by Eq. (22). The moving mass of the armature and the stiffness of springs are specified. The moving mass includes the armature, engine valve, keeper and a fraction of the springs. Table 3 shows the specifications of the mechanical subsystem.

$$m\ddot{x} + c\dot{x} + 2kx = F_{magnetic} \tag{22}$$

Initial condition $x(0) = 0$ mm, $\dot{x}(0) = 0$

Where:

m : moving mass (kg)
x : displacement of armature (m)
k : spring stiffness (N/m)
c : damping coefficient (N·s/m)
$F_{magnetic}$: the magnetic force (N)

The electrical subsystem consists of the coil, the shorted turn and the voltage power supply. The electrical subsystem is described by Eq. (23) and Table 4 shows the specifications of the electric subsystem.

Table 3. Physical properties of hybrid magnet engine valve actuator system.

Symbol	Magnitude
$2k$	29.2 (kN/m)
m	0.136(kg)
c	2.8182

Table 4. Specification of electic subsystem.

Quantity	Magnitude
Input initial Voltage	30 (V)
Number of turns	250 (turns)
Resistance	0.8886 (Ω)

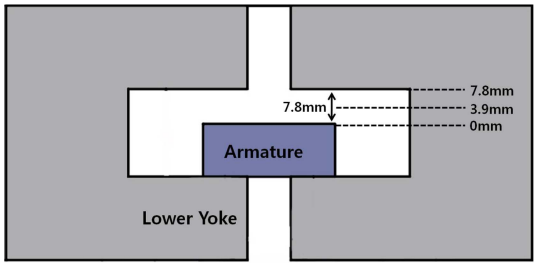

Fig. 7. (Color online) Schematic diagram of the armature position.

$$\frac{d\lambda(i,x)}{dt} + Ri = V \tag{23}$$

Initial condition $i(0) = 0$, $V(0) = 30$

Where:

λ : flux linkage (Wb·m)
i : coil electric current (A)
R : resistance of coil (Ω)

Fig. 7 shows the schematic diagram of the armature position. Thirty Volts was applied to the coil to move the armature from the lower end (0 mm) to the neutral position (3.9 mm). Then, –30 Volts was applied to move the armature from the neutral position to the upper end (7.8 mm).

A 2-D dynamic finite-element model, which consisted of 40,000 triangle elements, was created to assist in the modelling of these coupled systems. The dynamic motion of the armature from the lower end to the upper end of the stroke was simulated.

The analysis was performed in 1 μs time steps over a period of 5 ms. The magnetic forces exerting on the moving armature was computed by the virtual work principle method.

5. Results and Discussion

Fig. 8 shows the magnetic flux lines at three different positions during the motion of the armature. At both ends of the stroke, the magnetic force from the permanent magnet holds the armature, and at the mid- travel, the magnetic flux distribution is symmetric and the force acting on the armature cancelsout to zero.

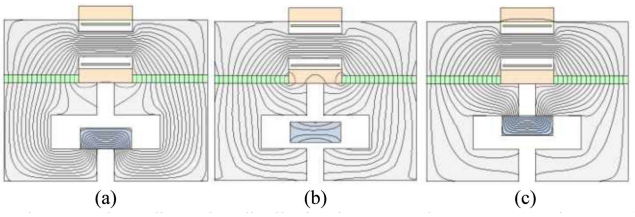

Fig. 8. (Color online) Flux distribution in proposed actuator (a) at lower end (b) at neutral position (c) at upper end.

Fig. 9 shows the graphs of the electric current versus time of the conventional actuator and the proposed actuator with the shorted turn. The electric current of the proposed actuator rises about 3 times faster than that of the conventional actuator. Fig. 10 shows the profiles of magnetic force and spring force versus time of the conventional and the proposed actuator, respectively. At the initial position, the magnetic force is larger than the spring force by 100 N. As the electromagnet is energized, the magnetic force is reduced but the spring force exceeds the magnetic force. The magnetic force of the proposed actuator equals the spring force at 0.01 ms because of the shorted turn whereas that of the conventional actuator equals the spring force at 1.77 ms because of the high inductance of the coil.

Fig. 11 shows the graphs of the armature position versus time of the conventional actuator and the proposed actuator, respectively. The armature of the proposed actuator is released 1.76 ms faster than that of the conventional actuator. The total transition time of the proposed actuator is 4.15 ms, which is 46% less than the total transition time of the conventional hybrid magnet engine valve actuator.

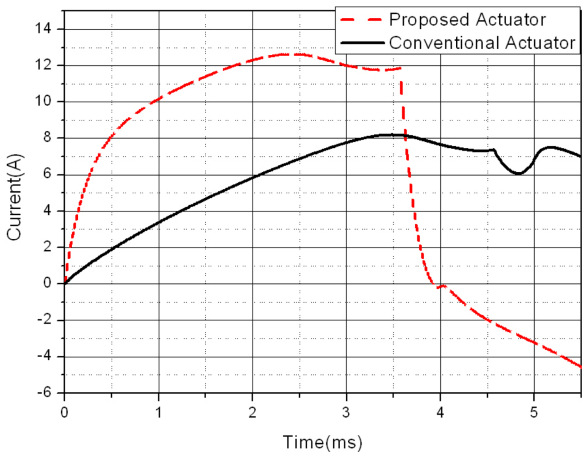

Fig. 9. (Color online) Comparison between conventional and proposed actuator for Electric current versus time.

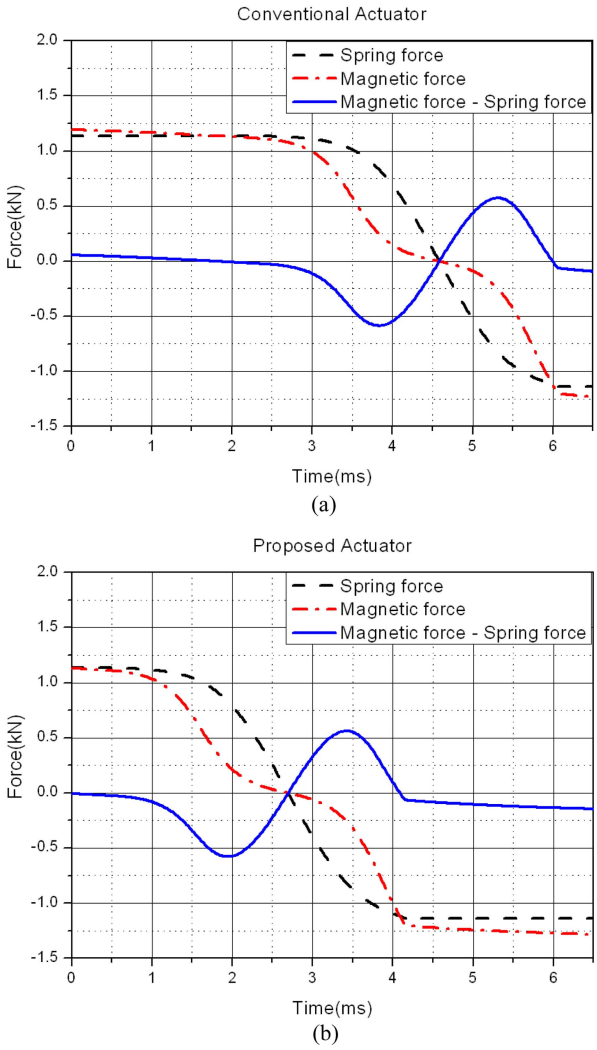

Fig. 10. (Color online) Force comparison of conventional and proposed actuator (a) conventional actuator (b) proposed actuator.

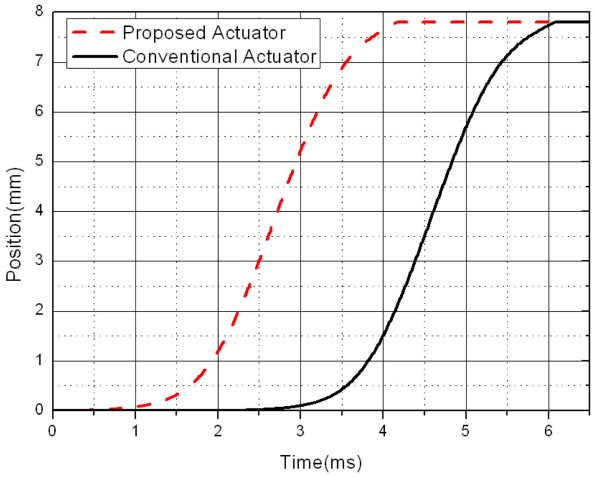

Fig. 11. (Color online) Position comparison of conventional and proposed actuator.

6. Conclusion

In this paper, a new design of a hybrid magnet engine valve actuator with a shorted turn is proposed. To verify the improved characteristics of the proposed hybrid magnet engine valve actuator, a lumped parameter analysis and a dynamic finite element analysis were performed.

Under an applied voltage, the shorted turn of the proposed actuator reduced the initial electric current rising time, making the electric current rise about 3 times faster than that of the conventional actuator, resulting in 46% faster transition of the armature.

Acknowledgment

This research was supported by Yeungnam University research grant in 2013.

References

[1] P. Barkan and T. Dresner, SAE Technical Paper Series (1989) p. 891676.
[2] M. Pischinger, W. Salber, F. Staay, H. Baumgarten, and H. Kemper, SAE Technical Paper Series (2000) p. 1223.
[3] M. Hamazaki and T. Hosaka, SAE Technical Paper Series (1991) p. 910008.
[4] W. S. Chang, T. A. Parlikar, M. D. Seeman, D. J. Perreault, J. K. Kassakian, and T. A Keim, IEEE Trans. Power Electron. Trans. (2002) pp. 109-118.
[5] J. Kim and D. K. Lieu, IEEE International Conference on Electric Machines and Drives (2005) pp. 1773-1779.
[6] J. Arthur Wagner, IEEE Trans. Magn. **18**, 1770 (1983).
[7] Y. Hirano, J. Naruse, and R. Tsuchiyama, IEEE Trans. Magn. **25**, 3073 (1989).
[8] C. Dong, IEEE Trans. Magn. **19**, 1689 (1983).
[9] H. D. Chai, San Jose State University.
[10] J. Kim and D. K. Lieu, Mechanical Science and Technology (2007) pp. 602-606.
[11] J. P. Wang, D. K. Lieu, W. L. Lorimer, and A. Hartman, IEEE Trans. Magn. **33**, 4092 (1997).